Theor Chem Acc (1997) 96:151–156

Theoretical
Chemistry Accounts

Solvent effects on the n→π* transition of pyrimidine in aqueous solution

Jiali Gao, Kyoungrim Byun

Department of Chemistry, State University of New York, Buffalo, NY 14260, USA

Received: 14 January 1997 / Accepted: 21 February 1997

Abstract. A hybrid quantum mechanical and molecular mechanical potential is used in Monte Carlo simulations to examine the solvent effects on the electronic excitation energy for the $n \rightarrow \pi^*$ transition of pyrimidine in aqueous solution. In the present study, the pyrimidine molecule is described by the semi-empirical AM1 model, while the solvent molecules are treated classically. Two sets of calculations are performed: the first involves the use of the pairwise three-point charge TIP3P model for water, and the second computation employs a polarizable many-body potential for the solvent. The latter calculation takes into account the effect of solvent polarization following the solute electronic excitation, and makes a correction to the energies determined using pairwise potentials, which neglects such fast polarization effects and overestimates the solute-solvent interactions on the Franck-Condon excited states. Our simulation studies of pyrimidine in water indicate that the solvent charge redistribution following the solute electronic excitation makes modest corrections (about -130 cm^{-1}) to the energy predicted by using pairwise potentials. Specific hydrogen bonding interactions between pyrimidine and water are important for the prediction of solvatochromic shifts for pyrimidine. The computed $n \rightarrow \pi^*$ blue shift is 2275 ± 110 cm^{-1}, which may be compared with the experimental value (2700 cm^{-1}) from isooctane to water.

Key words: Solvent effect – Pyrimidine – Hybrid quantum mechanical and molecular mechanical potential

1 Introduction

Solvent effects play an essential role in chemistry and biochemistry because most chemical reactions are carried out in solution, and processes related to life take place in aqueous environments. One of the most effective experimental approaches to probe solute-solvent interactions is through electronic spectroscopic methods by examining the observed spectral shifts of chromophores in various solvents [1]. Based on changes of electronic absorption spectra the solvent polarity may be defined, which provides a quantitative measure of the solvent's ability to polarize the solute's electronic structure. For example, one of the most widely used solvent polarity scales is the $E_T(30)$ values, which are determined from the solvatochromic shifts for the $n \rightarrow \pi^*$ transition of the pyridinium N-phenolate betaine dye in a variety of solvents [2, 3]. Thus, it is of interest to develop and refine theoretical methods that can predict solvent effects on the absorption energy of chromophores.

Continuum solvation models have been widely used, which provide useful quantitative and qualitative information [1, 4, 5]. Continuum methods have the advantage of computational efficiency because the solvent is characterized by a dielectric medium. Consequently, a great number of large molecules can be studied. The shortcoming, however, is a lack of specific consideration of hydrogen bonding interactions, which in certain cases need to be explicitly included. An example was recently provided by Karelson and Zerner [6], who showed that the $n \rightarrow \pi^*$ blue shift of pyrimidine in water can only be adequately predicted with the inclusion of two explicit water molecules that form hydrogen bonds to the two nitrogen atoms. Microscopic simulation techniques, on the other hand, can treat intermolecular interactions explicitly, and have been applied to the study of solvent effects on solvatochromic spectral shifts [7–10]. An attractive approach is a method that combines quantum mechanics (QM) with molecular mechanics (MM) to describe interactions between solute and solvent molecules [11, 12]. In such a hybrid QM/MM approach, the solute molecule is treated by QM methods, while the remainder of the system – the solvent molecules – are approximated by MM force fields. The method goes beyond the traditional force field calculations in that electronic properties, including bond formation and breaking, and the electronic absorption and emission spectra, can be addressed [12].

Application of hybrid QM/MM potentials to the investigation of solvatochromic shifts at the molecular

Correspondence to: J. Gao

level was pioneered by Warshel and coworkers [7]. We have also developed a hybrid QM-configuration interaction (CI) and MM method for the study of solvent effects on electronic excited states [8]. This method can yield good results for spectral shifts of acetone in aqueous and organic solvents, as well as for the prediction and interpretation of the excited state acidity constants (pK_a) of organic compounds in solution [8]. However, our early studies utilized an effective pair potential for the solvent, whose charge distribution does not respond to the variation of the solute's charge redistribution. Recently, Thompson and Schenter [13], presented a detailed description for coupling a polarizable MM force field with a QM method in molecular dynamics simulations, and have investigated the excited states of the bacteriochlorophyll-b dimer in the photosynthetic reaction center using an INDO/s QM Hamiltonian. The same technique has been described and implemented in our program [13, 14]. In this paper, we present results from a statistical Monte Carlo simulation of the pyrimidine n $\rightarrow \pi^*$ blue shift in aqueous solution using hybrid QM/MM potentials. The effect of the solvent polarization, in response to the solute electronic excitation, is approximated by using a polarizable MM solvent model [13, 14]. Below, the method and computational details employed in the present study are given, followed by results and discussion. The paper concludes with a summary of the major findings of this investigation.

2 Method

We employ a hybrid QM/MM potential in statistical mechanical Monte Carlo simulations to investigate the effect of aqueous solvation on the n $\rightarrow \pi^*$ absorption energy of pyrimidine. The method is based on a recently developed procedure, in which the chromophore molecule is treated with a CI wavefunction, and the surrounding solvent molecules with empirical potential functions [7, 8]. In previous studies, effective pairwise potentials have been used for the solvent. Thus, the charges of the solvent molecules are fixed [8]. Although in the Franck-Condon transition, the solvent nuclei do not have sufficient time to reorient and the excitation energy can be evaluated using the ground-state configuration, the solvent charge distribution must respond to the change of the solute wavefunction. The latter effect has been neglected with the use of pair potentials. A viable approach to take into account the solvent polarization effect in estimating electronic transition energies is to use a polarizable solvent model as originally described by Luzhkov and Warshel [7]. Thompson and Schenter [13] recently presented a detailed description of the computational procedure. Here, we employ the same approach to examine the magnitude of the polarization correction to the excitation energy estimated with the use of pair potentials [14]. Pyrimidine in water is chosen as a model system in the present study. The solvent effect on pyrimidine absorption spectra has received significant theoretical attention [6, 10, 15]. A recent systematic investigation by Zeng et al. [10] provides an excellent source of data for comparison.

The total energy of the hybrid system with the use of a polarizable solvent model can be written as follows [13, 14]:

$$E^g_{\text{tot}} = \langle \Phi^g_{CI}|\hat{H}^o_X + \hat{H}_{Xs}(\{q_s, \mu^g_s\})|\Phi^g_{CI}\rangle + E^{\text{pair}}_{ss} - \frac{1}{2}\sum_s \boldsymbol{\mu}^g_s \cdot \boldsymbol{E}^o_s + \frac{1}{2}\sum_s \boldsymbol{\mu}^g_s \cdot \boldsymbol{E}^{qm}_s(\Phi^g_{CI}) \quad (1)$$

where Φ^g_{CI} is the ground state CI wavefunction of the solute chromophore, $\hat{H}^o_X$ is the solute Hamiltonian, and $\hat{H}_{Xs}(\{q_s, \mu^g_s\})$ is the solute-solvent interaction Hamiltonian. In Eq. (1), E^{pair}_{ss} is the solvent pair interaction energy, consisting of both van der Waals and Coulombic terms, $\boldsymbol{\mu}^g_s$ is the solvent induced dipole moment in the presence of the ground-state solute, $\boldsymbol{E}^o_s$ is the electric field at position s due to the permanent solvent charges, and $\boldsymbol{E}^{qm}_s(\Phi^g_{CI})$ is the electric field exerted by the solute wavefunction. The Hamiltonian $\hat{H}_{Xs}(\{q_s, \mu^g_s\})$ consists of three terms [12–14]:

$$\hat{H}_{Xs}(\{q_s, \mu^g_s\}) = \hat{H}^{vdW}_{Xs} + \hat{H}^q_{Xs} + \hat{H}^{\mu}_{Xs}(\{\mu^g_s\}) \quad (2)$$

which represent, respectively, solute-solvent van der Waals, Coulombic, and charge-induced dipole interactions. Note that $\hat{H}^{\mu}_{Xs}(\{\mu^g_s\})$ is a function of the solvent-induced dipoles, whereas $\{\mu^g_s\}$ depends on the solute wavefunction via Eq. (3). Thus, $\{\mu^g_s\}$ and Φ^g_{CI} must be determined consistently in an iterative fashion.

$$\mu^g_s = \alpha_s[\boldsymbol{E}^o_s - \sum_{t\neq s} \boldsymbol{T}_{st} \cdot \boldsymbol{\mu}^g_t + \boldsymbol{E}^{qm}_s(\Phi^g_{CI})]. \quad (3)$$

Here, T_{st} is the standard dipolar tensor.

A similar expression can be obtained for the excited state of the solute, assuming that the solvent polarization instantaneously follows the solute electronic excitation, Eq. (4) [13]:

$$E^e_{\text{tot}} = \langle \Phi^e_{CI}|\hat{H}^o_X + \hat{H}_{Xs}(q_s, \mu^e_s)|\Phi^e_{CI}\rangle + E^{\text{pair}}_{ss} - \frac{1}{2}\sum_s \boldsymbol{\mu}^e_s \cdot \boldsymbol{E}^o_s + \frac{1}{2}\sum_s \boldsymbol{\mu}^e_s \cdot \boldsymbol{E}^{qm}_s(\Phi^e_{CI}). \quad (4)$$

In Eq. (4), the superscript e indicates that the solute molecule is in an electronically excited state, and $\boldsymbol{\mu}^e_s$ is the solvent-induced dipole in the presence of the excited solute molecule. $\boldsymbol{\mu}^e_s$ is obtained by replacing $\boldsymbol{E}^{qm}_s(\Phi^g_{CI})$ by $\boldsymbol{E}^{qm}_s(\Phi^e_{CI})$ in Eq. (3). The exact solution of Eq. (4) requires an iterative, self-consistent field (SCF) procedure, involving coupled QM-CI and MM polarization computations. To a first-order approximation, the procedure may be simplified by replacing the fully converged excited wavefunction with that obtained using the ground-state QM/MM dipole term [13]. Here, we indistinguishably use the notation Φ^e_{CI} to represent the two excited wave functions. Consequently, the QM/MM polarization term in Eq. (4) may be approximated as follows:

$$\langle \Phi^e_{CI}|\hat{H}^{\mu}_{Xs}(\{\mu^e_s\})|\Phi^e_{CI}\rangle \simeq \langle \Phi^e_{CI}|\hat{H}^{\mu}_{Xs}(\{\mu^g_s\})|\Phi^e_{CI}\rangle + \langle \Phi^e_{CI}|\hat{H}^{\mu}_{Xs}(\{\Delta\boldsymbol{\mu}_s\})|\Phi^e_{CI}\rangle \quad (5)$$

where $\Delta\boldsymbol{\mu}_s = \boldsymbol{\mu}_s^e - \boldsymbol{\mu}_s^g$. The last term in Eq. (5) can also be expressed classically for the interaction between solvent-induced dipoles with the solute QM electric field:

$$\langle \Phi_{CI}^e | \hat{H}_{Xs}^{\mu}(\{\Delta\boldsymbol{\mu}_s\}) | \Phi_{CI}^e \rangle = -\Delta\boldsymbol{\mu}_s \cdot \boldsymbol{E}_s^{qm}(\Phi_{CI}^e). \tag{6}$$

Making use of Eqs. (5) and (6), Eq. (4) is rewritten as follows:

$$\begin{aligned} E_{\text{tot}}^e = {} & \langle \Phi_{CI}^e | \hat{H}_X^o + \hat{H}_{Xs}(\{q_s, \mu_s^g\}) | \Phi_{CI}^e \rangle + E_{ss}^{\text{pair}} \\ & + \frac{1}{2}\sum_s [\boldsymbol{\mu}_s^e \cdot \boldsymbol{E}_s^{qm}(\Phi_{CI}^e) - \boldsymbol{\mu}_s^e \cdot \boldsymbol{E}_s^o] \\ & - \sum_s \Delta\boldsymbol{\mu}_s \cdot \boldsymbol{E}_s^{qm}(\Phi_{CI}^e). \end{aligned} \tag{7}$$

The difference between Eqs. (4) and (7) is that the former involves iterative QM-CI and solvent-polarization SCF calculations, whereas the latter only requires the MM-SCF iteration to obtain $\boldsymbol{\mu}_s^e$. In Eq. (7), excited state energies in the CI calculation are determined by using the ground-state, solvent-induced dipoles [13]. We note that, without using a polarizable potential for the solvent, only the first two terms survive in Eqs. 1 and 7. Consequently, the energy terms involving MM polarization energies may be used as a correction to the excitation energies determined with pairwise, non-polarizable potentials. In continuum solvation models, the solvent electronic polarization contribution to solvatochromic spectral shifts is often approximated with the use of the optical dielectric constant of the solvent [4].

In the explicit simulation study, the solute excitation energy in solution is written as follows:

$$\Delta E_{\text{tot}}^{g\to e} = E_{tot}^e - E_{tot}^g = \Delta E_{\text{stat}}^{g\to e} + \Delta E_{\text{pol}}^{g\to e} \tag{8}$$

with

$$\begin{aligned} \Delta E_{\text{stat}}^{g\to e} = {} & \langle \Phi_{CI}^e | \hat{H}_x^o + \hat{H}_{Xs}^o(\{q_s, \mu_s^g\}) | \Phi_{CI}^e \rangle \\ & - \langle \Phi_{CI}^g | \hat{H}_X^o + \hat{H}_{Xs}(\{q_s, \mu_s^g\}) | \Phi_{CI}^g \rangle, \end{aligned} \tag{9}$$

$$\begin{aligned} \Delta E_{\text{pol}}^{q\to e} = {} & -\frac{1}{2}\sum_s \Delta\boldsymbol{\mu}_s \cdot \boldsymbol{E}_s^o + \frac{1}{2}\sum_s \boldsymbol{\mu}_s^g \cdot \Big[\boldsymbol{E}_s^{qm}(\Phi_{CI}^e) \\ & - \boldsymbol{E}_s^{qm}(\Phi_{CI}^g)\Big] - \sum_s \Delta\boldsymbol{\mu}_s \cdot \boldsymbol{E}_s^{qm}(\Phi_{CI}^e). \end{aligned} \tag{10}$$

Here, $\Delta E_{\text{stat}}^{g\to e}$ represents the excitation energy obtained from hybrid QM/MM CI calculations using the static *ground-state solvent charge distribution*, and $\Delta E_{\text{pol}}^{g\to e}$ is a correction resulting from the instantaneous polarization of the solvent molecules following the solute excitation. The solvent spectral shift is defined as the difference of excitation energies in solution and in the gas phase, and is averaged over the Monte Carlo trajectory.

$$\langle \Delta v \rangle = \langle \Delta E_{\text{tot}}^{g\to e} \rangle - \Delta E_{\text{gas}}^{g\to e} = \langle \Delta\Delta E_{\text{stat}}^{g\to e} \rangle + \langle \Delta E_{\text{pol}}^{g\to e} \rangle \tag{11}$$

where the brackets indicate ensemble averages, and $\Delta\Delta E_{\text{stat}}^{g\to e} = \Delta E_{\text{stat}}^{g\to e} - \Delta E_{\text{gas}}^{g\to e}$.

3 Computational details

Statistical Monte Carlo simulations are carried out for a system containing 510 water molecules plus one pyrimidine in a cubic box with periodic boundary conditions. Two separate calculations are performed, in which the electronic structure of pyrimidine is represented by a CI wavefunction constructed from single excitations of an active space of six occupied and six unoccupied molecular orbitals from the semi-empirical AM1 wave function [16, 17]. The first calculation involves hybrid QM-CI/MM simulations using the pairwise, three-point charge TIP3P model for water [18], which yields values for $\Delta E_{\text{stat}}^{g\to e}$ [Eq. 9]. The second computation utilizes the POL2 polarizable model for water developed by Dang [19] to give the polarization correction, $\Delta E_{\text{pol}}^{g\to e}$ [Eq. 10]. In the latter calculation, only single-point energy evaluations are performed on configurations saved during the first simulation, which includes a total of 200 structures. Monte Carlo simulations are run in an isothermal-isobaric (NPT) ensemble at 25°C and 1 atm. Spherical cutoff distances of 9 and 10 Å are used to determine solvent-solvent and solute-solvent interactions. The van der Waals parameters for the QM atoms are those determined in previous studies, except nitrogen for which the σ value has been reduced to 2.3 Å [20].

In all calculations, the pyrimidine structure is held rigid at the optimized AM1 geometry in the gas phase. Although the solvent effect may alter the solute geometry slightly, its consequence on the absorption energies is not considered in the present study. The Monte Carlo simulations involve at least 10^6 configurations of equilibration, followed by 2×10^6 configurations for data averaging. Statistical errors are determined from averages of 5×10^4 configurations. New configurations are generated by translating a randomly selected molecule in all three cartesian directions, and rotating around a randomly chosen axis. The Owicki-Scheraga preferential sampling technique is employed to enhance the statistics near the solute, such that solvent moves are made proportional to $1/(R^2 + W)$, where $W = 350$ Å^2, [21]. Volume moves are attempted on every 1250 configurations. The ranges of moves are ± 0.15 Å for translation, $\pm 15°$ for rotation, and ± 300 Å^3 for volume moves. All simulations are performed on IBM RS6000 computers using the MCQUB program, [22] which is interfaced with the MOPAC program for electronic structure calculations [17].

4 Results and discussion

4.1 Pyrimidine-water complexes

We first examine the structure and energy of pyrimidine-water clusters, $C_4H_4N_2/(H_2O)_n n = 1, 2$, using Monte Carlo simulated annealing techniques. The initial configuration of the two complexes is generated by deleting all water molecules in the system for fluid simulations except one and two water molecules with the largest interaction energies. Then, the complex system is equilibrated for 10 000 configurations at 150 K, after

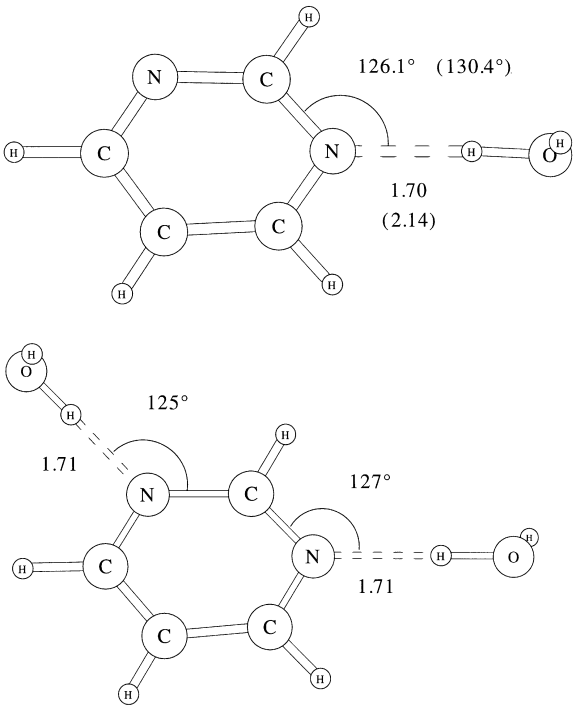

Fig. 1. Hydrogen bonding structures for pyrimidine-water complexes optimized from Monte Carlo simulated annealing at 0.1 K

which the system is continuously annealed to a temperature of 0.1 K in about 50 000 configurations. The final minimum structures are shown in Fig. 1, with key geometrical parameters listed.

Hydrogen-bonding energies for complexes with one and two water molecules are −4.7 and −9.0 kcal/mol, respectively, from the hybrid QM/MM calculation, which may be compared with the ab initio HF/6-31 + G(d)//6-31 + G(d) value of −5.2 kcal/mol for the pyrimidine-water bimolecular complex. In addition, the HF optimized structures are subjected to DFT/B3LYP/6-31 + G(d) single-point energy calculations, and an interaction energy of −5.9 kcal/mol is obtained. Thus, it appears that the present combined AM1/TIP3P model underestimates pyrimidine-water hydrogen bonding interactions by about 1 kcal/mol. In the present Monte Carlo simulated annealing optimizations, the water molecule prefers a tilted conformation with the non-bonding hydrogen pointing away from the pyrimidine symmetry plane. However, the ab initio calculations are performed with a C_s symmetry, having both water and pyrimidine constrained to the same plane. Zeng et al. [10] examined several empirical potential functions for pyrimidine, and found that Jorgensen's OPLS potential gives an interaction energy of −4.2 kcal/mol [23]. They noted that potential functions with partial charges derived from HF electrostatic potentials using double zeta plus polarization basis functions yield a much stronger binding energy of 7.5–8.9 kcal/mol, depending on the way in which QM electrostatic potentials are used to fit atomic charges [10]. For the singly bonded complex, a blue shift of 1235 cm^{-1} is obtained using the hybrid AM1-CIS/MM method. This turns out to be in agreement with the value of 1380 cm^{-1} predicted by Zeng et al.

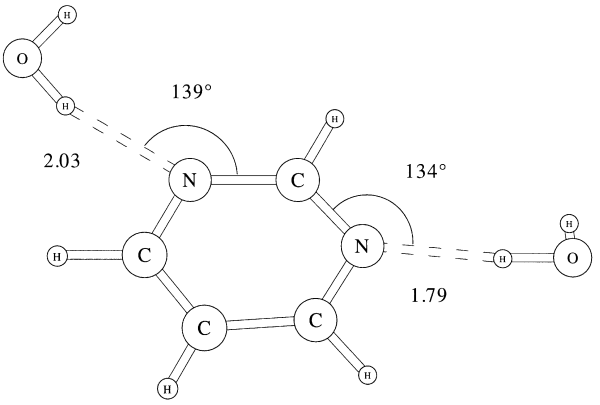

Fig. 2. Final structure from Monte Carlo simulations of the complex at 150 K

[10c]. Hydrogen bonding to a second water molecule further increases the excitation energy, resulting in a predicted blue shift of 2790 cm^{-1} at 0.1 K, which is as large as the entire experimental solvent spectral shifts [10]. However, as noted previously by Zeng et al. [10] hydrogen-bonding interactions with pyrimidine are rather flexible and can easily be distorted by thermal fluctuations as the temperature increases. For example, at 150 K, the average interaction energy for the $C_4H_4N_2/(H_2O)_2$ complex is reduced to −6.8 kcal/mol in hybrid QM/MM simulations, and the spectral shift for the $n \rightarrow \pi^*$ excitation is now about 1620 cm^{-1}. Interestingly, the two water molecules showed asymmetrical arrangement in the hydrogen-bonded complex at this temperature (Fig. 2). Karelson and Zerner [6] found that the excitation energy was red-shifted in the $C_4H_4N_2/(H_2O)_2$ complex using the INDO/S model, whereas the continuum dielectric effects increase the excitation energy of this tri-molecular complex. The reason that INDO/S yields red shifts is perhaps due to a particular choice of configurations in the CI calculation, although most configurations lead to blue shifts.

4.2 Solvatochromic shifts

The computed solvatochromic shifts and contributing components for pyrimidine in water are listed in Table 1. The $n \rightarrow \pi^*$ excitation energy is computed at 31 440 cm^{-1} using the AM1 CI-singles method, which may be compared with the INDO/S value of 32 966 cm^{-1}, [6] and the experimental excitation energy of 34 200 cm^{-1} for the $n \rightarrow \pi^*$ transition of pyrimidine in isooctane [24]. Studies have shown that there are little spectral shifts from the gas phase to non-polar organic solvents [25]. The computed absorption energies are in surprisingly good agreement with the experiment even though the AM1 model is not optimized for spectroscopic calculations. The computed total solvatochromic blue shift for pyrimidine in water, from the hybrid QM/MM Monte Carlo simulations at 25°C, is 2275 ± 110 cm^{-1}, of which 2405 ± 100 cm^{-1} is due to electrostatic stabilization of the ground state over the excited state ($\Delta\Delta E_{\text{stat}}^{g \rightarrow e}$), and -130 ± 37 cm^{-1} red shift is from changes in solvent

Table 1. Computed solvatochromic shifts and energy components of pyrimidine in water using the hybrid QM1-CIS/MM method at 25°C and 1 atm. Energies are given in cm^{-1} [a]

Energy	QM/MM	exp
ν, gas phase	31 440	34 200[b]
ν, aqueous	33 715 ± 110	36 900
$\Delta\nu$	2 275 ± 110	2 700 ± 300
$\Delta\Delta E_{stat}^{g\to e}$	2 405 ± 100	
ΔE_{Xs}	2 975 ± 175	
$\Delta\Delta E_{X}^{g\to e}$	−570 ± 200	
$\Delta E_{pol}^{g\to e}$	−130 ± 37	

[a] The calculation gives two close transitions at 31 440 and 32 620 cm^{-1}, both of which give similar spectral shifts. Only the lowest transition is listed here and used in the discussion. The two energies may be averaged and similar results are obtained. Similar findings have been observed by Karelson and Zerner using the INDO/S method [6]. All quantities are averages from Monte Carlo simulations

[b] Absorption energies are for pyrimidine in isooctane [23]

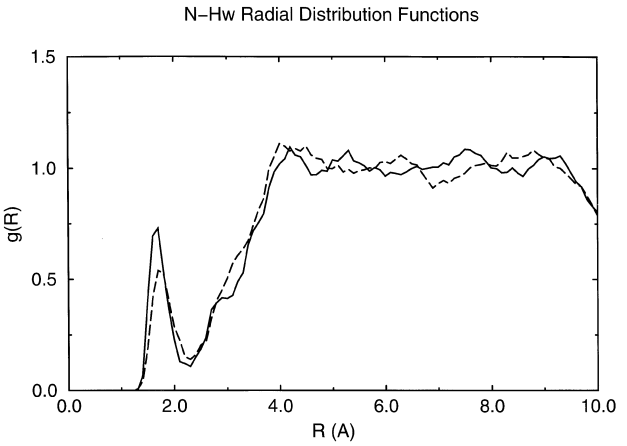

Fig. 3. Computed radial-distribution functions for the two pyrimidine nitrogen and the hydrogen of water at 25°C

polarization following the solute electronic transition ($\Delta E_{pol}^{g\to e}$). Analyzing various experimental studies, Zeng et al. concluded that the solvent shift of the absorption band center for pyrimidine in water is 2700 ± 300 cm^{-1} [10c, 24–26]. Thus, the present Monte Carlo simulations are in reasonable agreement with experiment. The difference may be attributed to weaker hydrogen-bonding interactions with water in the hybrid QM/MM treatment. On the other hand, the study by Zeng et al. [10c] employed classical dynamics simulations using partial charges fitted to the ground and excited-state electrostatic potentials, and over estimated the solvent shift by 700 cm^{-1}. In that work, hydrogen-bonding interactions were predicted to be 2–3 kcal/mol stronger than the B3LYP/6-31 + G(d) calculations. Clearly, details of the hydrogen-bonding strengths are critical for the prediction of solvatochromic shifts in simulation studies.

The origin of the computed solvatochromic spectral shift for pyrimidine in water is readily revealed by examining the components that contribute to the overall result (Table 1). As described in a previous study [8], the $\Delta\Delta E_{stat}^{g\to e}$ term can be separated into two components: (1) the change in solute-solvent interaction energy due to different solute charge distributions in the ground and excited state, ΔE_{Xs}, and (2) the change of the intrinsic excitation energy of the solute by solvation, $\Delta\Delta E_{X}^{g\to e}$. Following the solute electronic excitation, solute-solvent interactions are weakened by 8.5 ± 0.5 kcal/mol (2975 cm^{-1}) in the $n \to \pi^*$ transition. Along with the correction term resulting from the solvent polarization ($\Delta E_{pol}^{g\to e}$), differential solute-solvent interactions contribute 2845 cm^{-1} to the total spectral shift, because the ground state is better solvated than the excited state. Interestingly, the change in solvent polarization following the solute electronic excitation only makes a relatively small correction to the spectral shifts determined using an effective pairwise potential. Because the solute wavefunction is distorted in solution, the intrinsic energy gap between the ground and excited state is reduced by −570 cm^{-1} for the $n \to \pi^*$ transition.

The gas-phase dipole moment of pyrimidine from the AM1 calculation is 2.04 D, which is smaller than the experimental value (2.33 D) [27]. The average molecular dipole moment in water is estimated to be 2.93 ± 0.03 D in the present hybrid QM/MM Monte Carlo simulations. This represents a solvent-induced dipole moment of 0.89 D in water, in reasonable accord with the value of 0.7 D reported by Zeng et al. [10]. Solvent structural features for pyrimidine in water are illustrated by radial distribution functions (rdf) from hybrid QM/MM simulations. Figure 2 shows the rdf, g(R), for the N-H_w pairs, which provide an indication of the extent of specific hydrogen-bonding interactions. Hydrogen-bonding interactions are apparent from the strong first peaks in Fig. 3, similar to those observed by Zeng et al. [10c]. Integration to the minima revealed 1 and 0.8 water molecules in close contact with each of the two nitrogens, respectively. Thus, overall, there are an average of 1.7 water molecules forming specific hydrogen bonds with pyrimidine. Employing a set of electrostatic potential derived charges, Zeng et al. [10] also predicted strong hydrogen-bonding peaks in the N-H_w radial distribution function, amounting to two hydrogen bonds, one to each nitrogen atom in pyrimidine. These observations are consistent with the finding by Karelson and Zerner [6], who identified that two explicit water molecules are needed in continuum SCRF calculations in order to reproduce the experimental spectral shifts.

5 Conclusions

Hybrid QM/MM Monte Carlo simulations have been carried out to examine the solvatochromic shifts of pyrimidine in aqueous solution. In this study, the solvent polarization contribution following the solute electronic excitation is included. The computed $n \to \pi^*$ blue shift for pyrimidine in water is 2275 ± 110 cm^{-1}, in reasonable agreement with the experimental results (2700 ± 300 cm^{-1}) and with previous computational studies [6, 10]. Specific hydrogen-bonding interactions between pyrimidine and solvent play an essential role in

the solvent-induced spectral shifts. Analyses of solute-solvent interaction energies reveal that the solvent stabilizes the ground state more than the excited state by 8.5 kcal/mol, or 2975 cm^{-1}. Other factors contribute to a minor extent, with only -130 cm^{-1} from the solvent polarization correction.

Acknowledgements. We thank the National Science Foundation for support of this research and the referee for helpful comments.

References

1. Reichardt C (1990) Solvents and solvent effects in organic chemistry. VCH, Weinheim
2. Reichardt C (1994) Chem Rev 94:2319
3. Laurence C, Nicolet P, Dalati MT, Abboud J-LM, Notario R (1994) J Phys Chem 98:5807
4. (a) McRae EG (1957) J Phys Chem 61:562; (b) Bayliss NS (1950) J Chem Phys 18:292; (c) Lippert E (1970) Acc Chem Res 3:74; (d) Rosch N, Zerner MC (1994) J Phys Chem 98:5817; (e) de Vries AH, van Duijnen PT (1996) Int J Quantum Chem 57: 1067
5. For recent review, see (a) Tomasi J, Persico M (1994) Chem Rev 94:2027; (b) Cramer CJ, Truhlar DG (1995) In: Lipkowitz KB, Boyd DB (eds) Reviews in computational chemistry, vol 6 VCH, New York, pp 1–72
6. Karelson M, Zerner MC (1990) J Am Chem Soc 112:9405
7. (a) Luzhkov V, Warshel A (1991) J Am Chem Soc 113:4491; Warshel A (1979) J Phys Chem 83:1640
8. (a) Gao J (1994) J Am Chem Soc 116:9324; (b) Gao J, Li N, Freindorf M (1995) J Am Chem Soc 118:4912
9. (a) Debolt SE, Kollman PA (1990) J Am Chem Soc 112:7515; (b) Blair JT, Krogh-Jespersen K, Levy RM (1989) J Am Chem Soc 111:6948; (c) Zeng J, Woywod C, Hush NS, Reimer JR (1995) J Am Chem Soc 117:8618; (d) Zeng J, Hush NS, Reimer JR (1996) J Phys Chem 100:9561
10. (a) Zeng J, Craw JS, Hush NS, Reimers JR (1993) J Chem Phys 99:1482; (b) Zeng J, Hush NS, Reimers JR (1993) J Chem Phys 99:1496; (c) Zeng J, Hush NS, Reimers JR (1993) J Chem Phys 99:1508
11. (a) Warshel A, Levitt M (1976) J Mol Biol 103:227; (b) Field MJ, Bash PA, Karplus M (1990) J Comput Chem 11:700; (c) Singh UC, Kollman PA (1986) J Comput Chem 7:718; (d) Topia O, Colonna F, Angyan JG (1990) J Chem Phys 87:875; (e) Gao J (1992) J Phys Chem 96:537
12. For a review, see Gao J (1995) In: Lipkowitz KB, Boyd DB, (eds) Reviews in computational chemistry, vol 7. VCH, New York, pp 119–185
13. (a) Thompson MA, Schenter GK (1995) J Phys Chem 99:6374; (b) Thompson MA (1996) J Phys Chem 100:14492
14. Gao J (1997) J Comput Chem 18:1061
15. (a) Del Bene JE, (1975) J Am Chem Soc 112:9405; (b) Del Bene JE (1976) J Chem Phys 15:463
16. Dewar MJS, Zoebisch EG, Healy EF, Stewart JJP (1985) J Am Chem Soc 107:3902
17. (a) Stewart JJP (1990) J Comput Aided Mol Des 4:1; (b) Stewart JJP (1986) MOPAC version 5, Quantum chemistry program exchange 455, vol 6, No. 391
18. Jorgensen WL, Chandrasekhar J, Madura JD, Impey RW, Klein ML (1983) J Chem Phys 79:926
19. Dang LX (1992) J Chem Phys 97:2659
20. Gao J, Xia X (1992) Science 258:631
21. (a) Owicki JC, Scheraga HA (1977) Chem Phys Lett 47:600; (b) Owicki JC (1978) ACS Symp Ser no 86, 159
22. Gao J (1996) MCQUB. State University of New York, Buffalo
23. Jorgensen WL, Briggs JM, Contreras ML (1990) J Phys Chem 94:1683
24. (a) Baba H, Goodman L, Valenti PC (1996) J Am Chem Soc 88:5411; (b) Cohen BJ, Baba H, Goodman L (1965) J Chem Phys 43:2902
25. (a) Carrabba MM, Kenny JE, Moomaw WR, Cordes J, Denton M (1985) J Phys Chem 89:674; (b) Innes KK, McSwiney HD Jr, Simmons JD, Tilford SG (1969) J Mol Spectrosc 31:76; (c) Pisanias MN, Christophorou LG, Carter JG, McCorkle DL (1972) J Chem Phys 58:2110
26. Borresen HC (1963) Acta Chem Scand 17:921
27. McClellan AL (1989) Tables of experimental dipole moments. Rahara Enterprises, El Cerrito, Calif